Cubic N-vector model and randomly dilute Ising model in general dimensions

Kathie E. Newman* and Eberhard K. Riedel

Department of Physics, University of Washington, Seattle, Washington 98195

(Received 29 June 1981)

Critical properties of models defined by continuous-spin Landau Hamiltonians of cubic symmetry are calculated as functions of spatial dimensionality, $2.8 \leq d \leq 4$, and number of spin components, N. The investigation employs the scaling-field method developed by Golner and Riedel for Wilson's exact momentum-space renormalization-group equation. Fixed points studied include the isotropic and decoupled Ising ($-2 \leq N < \infty$), the face- and corner-ordered cubic ($1 \leq N < \infty$), and, via the replica method for $N \rightarrow 0$, the quenched random Ising fixed point. Variations of N and d are used to link the results to exact results or results from other calculational methods, such as ϵ expansions near two and four dimensions. This establishes the consistency of the calculation for three dimensions. Specifically, truncated sets involving seven (twelve) scaling-field equations are derived for the cubic N-vector model. A stable random Ising fixed point is found and shown to be distinct from the cubic fixed point and to connect, as a function of d, with the Khmelnitskii $\epsilon^{1/2}$ fixed point. At $d = 3$, the short truncation yields $\alpha \approx 0.11$ for the pure Ising and $\alpha \approx -0.09$ for the random Ising fixed point. A search for a random tricritical fixed point was inconclusive. For the N-component cubic model, the spin dimensionality N_c, at which the isotropic and cubic fixed points change stability, is determined as a function of d. The results support $N_c > 3$ for three dimensions.

I. INTRODUCTION

Anisotropic N-vector models of cubic symmetry have played an important role in the development of the renormalization-group (RG) approach to critical phenomena.[1,2] These models exhibit different types of continuous and first-order phase transitions, depending upon the number of spin components N, spatial dimension d, and sign and strength of the cubic coupling constant v.[3-6] Cubic models are widely applied to the study of magnetic and structural phase transitions[7,8] and, by means of the replica method, also to critical phenomena of randomly dilute Ising systems.[9-12] Many of these topics have been addressed by ϵ-expansion techniques near four and two dimensions[3-6] or by position-space methods in two dimensions.[13-15] In the present paper the *three-dimensional* random Ising and N-component cubic models are investigated by the scaling-field method based on Wilson's exact RG equation for critical phenomena.[16-18] The approach has been used previously to obtain accurate estimates for the critical exponents of the isotropic N-vector model in three dimensions.[17] Preliminary work on the cubic

model has also been reported.[19] Here the continuous-spin cubic model is investigated for general N and the range of dimensions $2.8 \leq d \leq 4$ in an approximation employing seven scaling-field equations. The main results are as follows. For the random Ising model a stable random fixed point is found for $2.8 \leq d \leq 4$. It connects near four dimensions with the $\epsilon^{1/2}$ Khmelnitskii fixed point[10,11] and is distinct from the analytic continuation in N of the cubic fixed point. We infer that the random Ising (RI) specific-heat exponent satisfies $\alpha^{RI} < 0$ for $2 < d < 4$, consistent with the proposed generalized Harris criterion.[20] At $d = 3$, the truncation yields $\alpha^I = 0.11$ and $\alpha^{RI} = -0.09$ for the pure and random Ising transitions. For the cubic model, the fixed-point structure and critical exponents are obtained as functions of N and d. The results confirm most qualitative conclusions drawn from ϵ-expansion work. The critical value N_c, at which the isotropic N-vector fixed point becomes unstable against cubic perturbations, is $3 < N_c < 4$ at $d = 3$. Differences between the continuous and discrete-spin cubic models are also discussed.

The continuous-spin cubic model is defined by the Landau Hamiltonian, $\beta \mathcal{H} = H[\sigma]$,

$$H[\sigma] = \frac{1}{2} \int_{\vec{q}} u_2(q)\vec{\sigma}(q)\cdot\vec{\sigma}(-q) + \frac{1}{4!} \int_{\vec{q}_1,\ldots,\vec{q}_4} \delta(\vec{q}_1 + \ldots + \vec{q}_4) \sum_{\alpha,\beta} (u_4\{\vec{q}_i\} + v_4\{\vec{q}_i\}\delta_{\alpha\beta})\sigma_\alpha(q_1)\sigma_\alpha(q_2)\sigma_\beta(q_3)\sigma_\beta(q_4)$$

$$+ \frac{1}{6!} \int_{\vec{q}_1,\ldots,\vec{q}_6} \delta(\vec{q}_1 + \cdots + \vec{q}_6) \sum_{\alpha,\beta,\gamma} (u_6\{\vec{q}_1\} + v_6\{\vec{q}_i\}\delta_{\alpha\beta} + w_6\{\vec{q}_i\}\delta_{\alpha\beta\gamma})$$

$$\times \sigma_\alpha(q_1)\sigma_\alpha(q_2)\sigma_\beta(q_3)\sigma_\beta(q_4)\sigma_\gamma(q_5)\sigma_\gamma(q_6) + \cdots . \tag{1.1}$$

The $\vec{\sigma}$ denote continuous N-component "spins," $\vec{\sigma} = \{\sigma_\alpha; \alpha = 1, \ldots, N; -\infty < \sigma_\alpha < \infty\}$, the $\vec{q}$-momentum vectors in d dimensions, and $\int_{\vec{q}} = \int d^d q$. For brevity we denote $u = u_4\{\vec{q}_i = 0\}$ and $v = v_4\{\vec{q}_i = 0\}$. The latter parameter, v, determines the symmetry and strength of the local cubic field. When $v < 0$ $(v > 0)$ the spins $\vec{\sigma}$ have a preferred orientation towards the faces (corners) of an N-dimensional hypercube. The parameter space of the Hamiltonian (1.1) encompasses isotropic $(u > 0, v = 0)$, face-ordered cubic $(u > 0, v < 0)$, corner-ordered cubic $(u > 0, v > 0)$, and decoupled Ising behaviors $(u = 0, v > 0)$, as well as, in the replica limit $N \to 0$, the weakly dilute Ising $(u < 0, v > 0)$ behavior.

The scaling-field method, which is applied here to the model (1.1), is particularly appropriate for the investigation of critical phenomena exhibiting crossover phenomena.[17] The approach starts from the representation of Wilson's exact functional-differential RG equation[16,18] in terms of an infinite set of ordinary differential equations. The method is versatile in that exponents and scaling functions can be computed. Furthermore, critical parameters such as N_c can be estimated directly for three dimensions. Approximations are generated by truncation. The difficulty in considering large truncations lies mainly in the labor of computing certain classes of coupling coefficients. However, for studies not aimed at high precision, such as the present one, relatively short truncations can be used that still ensure good estimates for the asymptotic critical-point exponents; the quality of the calculation is optimized by adjusting a scale parameter. Our study of the cubic model (1.1) uses a truncation including the seven most important "isotropic" and "cubic" scaling fields. The operator basis is chosen so that the number of spin components N and dimension d can be varied continuously. This makes accessible the replica limit $N = 0$, and allows one to test the method in limits in which exact results are available.

The discrete-spin cubic model[8,13] with a "face-ordered" cubic ground state is known to exhibit

additional features not contained in (1.1). The model is defined in terms of dipole and quadrupole nearest-neighbor interactions $v(\vec{S}\cdot\vec{S}') + w(\vec{S}\cdot\vec{S}')^2$, with $\vec{S}$ assuming the $2N$ values $(\pm 1, 0, 0, \ldots)$, $(0, \pm 1, 0, \ldots), \ldots$. It exhibits either one or two phase transitions, depending on the relative size of the coupling constants, and a point of $2N$-state Potts symmetry when $v = w$.[13] This behavior is exemplified by the Ashkin-Teller model[21] to which the discrete cubic model reduces at $N = 2$. For such models, as well as experimental systems, Landau Hamiltonians can be constructed by the Hubbard transformation[22] and group-theoretical methods.[23] The discrete N-component cubic model is equivalent to the Landau Hamiltonian (1.1) only when $v \gg w$, then exhibiting a single-phase transition. In general, the Landau expansion contains symmetry-breaking terms of both cubic and Potts symmetry.[14]

Similar observations can be made with regard to the replica representation of an Ising model containing quenched nonmagnetic impurities. By constructing first the Landau expansion for the discrete randomly dilute Ising model and then applying the replica method, one is led to Hamiltonian (1.1) for the quadrant $(u < 0, v > 0)$.[11] Obviously, this model does not describe the expected percolation transition at zero temperature. Interchanging the order in which the Hubbard transformation and replica method are applied, a Landau Hamiltonian in terms of a $(2^N - 1)$-component order parameter is obtained, which in the replica limit $N \to 0$ describes percolation through the one-state Potts model.[12,24] For general N, this Landau Hamiltonian is probably equivalent to that of the discrete-spin cubic model with "corner-ordered" ground states. The latter model is not well studied for general parameters but is known to reduce to a 2^N-state Potts model when all coupling constants are equal.[25] Our work is restricted to the weakly dilute Ising systems for which the model (1.1) with N-component order parameter is appropriate.

The outline of the paper is as follows. In Sec. II the scaling-field formalism is described and equa-

tions derived. Details are deferred to Appendices A and B. Results for the random Ising and N-component cubic models are given in Sec. III. Section IV presents a summary and discussion.

II. THE SCALING-FIELD METHOD

Wilson has proposed an exact differential RG equation that determines the evolution of the Landau Hamiltonian $H_l[\sigma]$ as a function of the RG iteration parameter l [see Eq. (11.17) of Ref. 16]. This equation has been transformed into an infinite hierarchy of ordinary differential equations.[17] Under the assumption that the eigenfunctionals $Q_m[\sigma]$ with scaling indices y_m provide a basis in the space of RG Hamiltonians, we expand $H_l[\sigma]$,

$$H_l[\sigma] = H^*[\sigma] + \sum_m \mu_m(l)Q_m[\sigma] , \qquad (2.1)$$

where $H^*[\sigma]$ denotes the fixed-point Hamiltonian. Substituting this expansion into the Wilson equation and projecting all terms onto the basis $Q_m[\sigma]$ yields the infinite set of coupled differential equations

$$\frac{d\mu_m}{dl} = y_m \mu_m + \sum_{j,k} a_{mjk}\mu_j\mu_k + \sum_j a_{mj}\mu_j + a_m . \qquad (2.2)$$

The μ_m are referred to as scaling fields and Eq. (2.2) as the scaling-field representation of the Wilson equation. The coupling coefficients a_{mjk}, a_{mj}, and a_m can be calculated when Gaussian eigenfunctionals are used as an operator basis. Via these coefficients the RG equations (2.2) depend on dimension d, number of spin components N, and spin-rescaling parameter Δ (in Wilson and Kogut's[16] notation, $\Delta \equiv 1 - d\rho/dl$). The latter parameter plays a crucial role in the RG transfor-

mation. Its fixed-point value Δ^* determines the correlation-function exponent η,

$$\eta = 2\Delta^* , \qquad (2.3)$$

and the origin of the spectrum of eigenvalues associated with the fixed point. Equation (2.2) is the starting point of the scaling-field method.

The expansion (2.1) for the cubic Landau Hamiltonian (1.1) requires all Gaussian eigenfunctions of isotropic and cubic symmetry. The pertinent formulas are summarized below. The Gaussian fixed point is[16]

$$H_G^*[\sigma] = \frac{1}{2} \int_{\vec{q}} u_G^*(q)\vec{\sigma}(q)\cdot\vec{\sigma}(-q) , \qquad (2.4)$$

where $u_G^*(q) = Aq^2/[Aq^2 + \exp(-2q^2)]$, A being a normalization parameter. The Gaussian eigenfunctionals $Q_m[\sigma]$ and eigenvalues y_m^G follow from the linearized Wilson equation. The $Q_m[\sigma]$ are polynomials in spins σ_α, $\alpha = 1, \ldots, N$, and momenta $\vec{q}$, with the momentum dependence being expressed in terms of a set of homogeneous functions of momentum of order p, $f_p\{\vec{q}\}$. The isotropic and cubic functionals are labeled by indices $\bar{m}, \bar{l}$ describing the degree in $(\vec{\sigma}\cdot\vec{\sigma})^{1/2}$ and σ_α, respectively, plus indices such as p characterizing momentum dependence. The eigenvalues y_m^G and eigenfunctionals $Q_m[\sigma]$ are given by[18]

$$y_{\bar{m}\bar{l};p}^G \ldots = d - \frac{1}{2}(\bar{m}+\bar{l})(d-2) - p \qquad (2.5)$$

and

$$Q_{\bar{m}\bar{l};p} \ldots [\sigma] = e^{-P}\bar{Q}_{\bar{m}\bar{l};p\ldots}[\sigma] , \qquad (2.6)$$

where

$$e^{-P} = \exp\left[-\frac{1}{2} \int_{\vec{q}} [u_G^*(q)]^{-1} \frac{\delta}{\delta\vec{\sigma}(q)} \cdot \frac{\delta}{\delta\vec{\sigma}(-q)} \right] \qquad (2.7)$$

and

$$\bar{Q}_{\bar{m}\bar{l};p}\ldots[\sigma] = \frac{1}{(\bar{m}+\bar{l})!} \int_{\vec{q}_1,\ldots,\vec{q}_{\bar{m}+\bar{l}}} f_{\bar{m}\bar{l};p}\ldots(\vec{q}_1,\ldots,\vec{q}_{\bar{m}+\bar{l}})\delta\left[\sum_{i=1}^{\bar{m}+\bar{l}}\vec{q}_i\right]\prod_{i=1}^{\bar{m}+\bar{l}}\psi(q_i)R_{\bar{m}\bar{l}}[\sigma(q_1),\ldots,\sigma(q_{\bar{l}+\bar{m}})] . \qquad (2.8)$$

Momentum integrals extend over all space and are effectively cut off by the factors of $\psi(q)$,

$$\psi(q) = \{u_G^*(q)[1 - u_G^*(q)]/Aq^2\}^{1/2}$$
$$= e^{-q^2}/(Aq^2 + e^{-2q^2}) .$$

The forms of this auxiliary function and of $u_G^*(q)$

are the result of Wilson's choice of the "incomplete integration" procedure for the RG elimination of degrees of freedom. The momentum dependence through $\psi(q)$ remains even for functionals with $p = 0$, for which $f_{\bar{m}\bar{l};p=0}\{\vec{q}\} = 1$. The isotropic eigenfunctionals are defined by

$$R_{\bar{m}0}[\sigma]=\prod_{i=1}^{\bar{m}/2}\vec{\sigma}(q_{2i-1})\cdot\vec{\sigma}(q_{2i}) ,$$ (2.9)

and the cubic eigenfunctionals to order σ^8 (written without momentum dependence on the spin variables) by

$$R_{04}[\sigma]=(N-1)\sum_{\alpha}\sigma_{\alpha}^4-6\sum_{\alpha<\beta}\sigma_{\alpha}^2\sigma_{\beta}^2 ,$$ (2.10a)

$$R_{24}[\sigma]=\left[\sum_{\alpha}\sigma_{\alpha}^2\right]R_{04}[\sigma] ,$$ (2.10b)

$$R_{06}[\sigma]=(N-1)(N-2)\sum_{\alpha}\sigma_{\alpha}^6-15(N-2)\sum_{\alpha\neq\beta}\sigma_{\alpha}^4\sigma_{\beta}^2+180\sum_{\alpha<\beta<\gamma}\sigma_{\alpha}^2\sigma_{\beta}^2\sigma_{\gamma}^2 ,$$ (2.10c)

$$R_{44}[\sigma]=\left[\sum_{\alpha}\sigma_{\alpha}^2\right]^2 R_{04}[\sigma] ,$$ (2.10d)

$$R_{26}[\sigma]=\left[\sum_{\alpha}\sigma_{\alpha}^2\right]R_{06}[\sigma] ,$$ (2.10e)

$$R_{08}[\sigma]=(N-1)\sum_{\alpha}\sigma_{\alpha}^8-28\sum_{\alpha\neq\beta}\sigma_{\alpha}^6\sigma_{\beta}^2+70\sum_{\alpha<\beta}\sigma_{\alpha}^4\sigma_{\beta}^4$$ (2.10f)

$$R_{044}[\sigma]=\tfrac{1}{2}(N-2)(N-3)\sum_{\alpha<\beta}\sigma_{\alpha}^4\sigma_{\beta}^4-6(N-3)\sum_{\alpha<\beta<\gamma}\{\sigma_{\alpha}^2\sigma_{\beta}^2\sigma_{\gamma}^4+\sigma_{\alpha}^2\sigma_{\beta}^4\sigma_{\gamma}^2+\sigma_{\alpha}^4\sigma_{\beta}^2\sigma_{\gamma}^2\}$$

$$+108\sum_{\alpha<\beta<\gamma<\delta}\sigma_{\alpha}^2\sigma_{\beta}^2\sigma_{\gamma}^2\sigma_{\delta}^2 .$$ (2.10g)

In Eq. (2.8), $R_{\bar{m}l}\equiv R_{\bar{m},l_1,\ldots,l_t}$, where t denotes the number of nonzero $\bar{l}_i$ needed to specify the cubic eigenfunctionals (i.e., $t=1$ for $R_{\bar{m};4}$, $R_{\bar{m};6}$, $\ldots$, and $t=2$ for $R_{\bar{m};44}$, $\ldots$, etc.). The operators are traceless, satisfying

$$\sum_{\alpha=1}^{N}\left[\frac{\delta}{\delta\sigma_{\alpha}}\right]^2 R_{\bar{m}l}[\sigma]=0 .$$

For given $\bar{l}=\bar{l}_1+\bar{l}_2+\cdots+\bar{l}_t$ the number of independent cubic eigenfunctionals depends on N.[26] However, with the choice of eigenfunctionals (2.10) it is not necessary to adjust the basis as N is changed. In the resulting scaling-field equations N can be varied continuously between -2 and ∞. At each integer value of N the equations for the superfluous μ_m decouple from the set. The coupling coefficients in Table I of Appendix A exhibit this feature.

The scaling-field equations (2.2) for the cubic model are derived by computing the coupling coefficients a_{mjk}, a_{mj}, and a_m, where $m=\{\bar{m},\bar{l};p,\ldots\}$. These coefficients are calculated by means of an operator-product expansion. Details are given in Appendix A. Here we remark only that the a_{mjk} are projections of terms involving products of Q_j and Q_k onto Q_m, while the a_{mj} are those of terms involving Q_j and a_m of a term projecting only onto

the eigenfunctional $Q_{20;2}$. The coefficients are products of combinatorial factors involving N and momentum integrals depending on dimension d and spin-rescaling parameter Δ. The evaluation of the integrals is also discussed in Appendix A. Finally, two scale changes are applied to the scaling-field equations. One amounts to a change in the normalization of the integrals and is defined by Eq. (A15). The other is necessary for properly taking the limit $N\to\infty$. In Eqs. (2.9) and (2.10) the $R_{\bar{m}l}$ are replaced by

$$\bar{R}_{\bar{m}l}=N^{-\bar{m}/2-\phi_l}R_{\bar{m}l} ,$$ (2.11)

where $\phi_l\equiv\phi_{l_1,\ldots,l_t}$ equals the order in N of $R_{0,l_1,\ldots,l_t}$; that is, $\phi_4=\phi_8=2$, $\phi_6=3$, $\phi_{44}=4$. A compensating scale change in the scaling fields,

$$\bar{\mu}_{\bar{m}l;p}\cdots=N^{\bar{m}/2+\phi_l-1}\mu_{\bar{m}l;p}\cdots$$ (2.12)

is made so that each term in Eq. (2.1) is order $1/N$. This scale factor is absorbed in the new coupling coefficients $\bar{a}_{mjk}$, $\bar{a}_{mj}$, and $\bar{a}_m$ displayed in Eq. (A14). We have adopted the convention of working with the equations for μ_m when $N<1$, and for $\bar{\mu}_m$ when $N\geq 1$.

The principal steps in applying the scaling-field formalism are the following. First, approximations

are generated by truncating the infinite hierarchy of equations. The cubic model has been discussed primarily for a truncation that includes the isotropic scaling fields $\overline{ml};p =20;0, 40;0, 60;0,$ and $20;2$ and the cubic scaling fields $04;0, 24;0,$ and $06;0$. For simplicity the label $p =0$ is deleted and the notation used is $\overline{ml}=20, 40, 60,$ and $2'0$ for the isotropic scaling fields and $\overline{ml}=04, 24,$ and 06 for the cubic scaling fields. All coupling coefficients for this truncation are given in Appendix A. It amounts to including all terms of order σ^6 with $p =0$ in the expansion (2.1). For investigating random tricritical behavior the truncation was extended to include also the isotropic field 80 and the cubic fields 08, 26, 44, and 044. Criteria for generating "balanced" truncations were developed in a study of the isotropic N-vector model.[27] It was found that high-precision calculations require a substantial number of fields conjugate to eigenfunctionals $Q[\sigma]$ of higher-order momentum dependence, i.e., characterized by $f_p\{\vec{q}\}$ with $p \geq 2$. From this point of view the second truncation is less balanced than the first one.

Second, truncated sets of scaling-field equations are investigated either numerically or by expansion techniques. In both approaches d and N are varied continuously. For numerical studies the coupling coefficients are calculated for the dimension d of the system under consideration rather than being expanded about an upper critical dimension d^*. The range $2.8 \leq d \leq 4$ was studied. Whereas results from exact expansions are independent of redundant parameters such as the normalization A in Eq. (2.4), this is not the case for results from truncated sets of equations.[28] The parameter A is adjusted so that the truncation gives good results for the exponents of the isotropic N-vector model; $A =0.5$ is used.

Third, extracting information from the scaling-field equations involves the usual determination of the physical fixed points and their critical exponents and domains of attraction. This locates the critical and tricritical transitions. The identification of first-order (or critical end-point) behavior in momentum-space RG calculations uses the idea of "runaway" flows.[5,29] We identify as regions of first-order transitions, domains of the RG phase-transition surface not attracted by fixed points.

Fourth, a rule is required for determining the fixed-point value Δ^* of the spin-rescaling parameter Δ. The Δ^* yields the exponent η via Eq. (2.3). A theorem by Wegner[18] states that associated with fixed points, $d\mu_m^*/dl =0$ for all m, that exist only

for *discrete* values of Δ is a redundant operator Q_κ with scaling exponent y_κ. For example, the Gaussian fixed point (2.4), for which $\Delta_G^* =0$, has the marginal redundant operator $Q_{2'0}[\sigma]$. It has a simple interpretation. The equation

$$\frac{\partial H_G^*[\sigma]}{\partial A} = Q_{2'0}[\sigma] \tag{2.13}$$

shows that shifts in the scaling field $\mu_{2'0}^*$ are equivalent to changes in the physically redundant normalization constant A.[28] The physical critical exponents are constant along the line of Gaussian fixed points parametrized by A.[27] In contrast, for truncated sets of RG equations critical fixed-point solutions are found for a *range* of values of Δ. Searching for a criterion that singles out one of these values we choose the condition

$$y_{2'0}(\Delta^*) =0 . \tag{2.14}$$

There the truncation exhibits not only a marginal redundant operator but also a vestige of the "line" of fixed points of the untruncated equations. This is seen from the fact that the quantity $d\mu_{2'0}/d\Delta$ diverges at $\Delta=\Delta^*$; that is, fixed points are localized in the plane $\Delta=\Delta^*$. When the numerical method employing (2.14) is applied to dimensions $d =4-\epsilon$, the ϵ-expansion result for η is reproduced.

III. RESULTS

Results of the scaling-field technique for the randomly dilute Ising and N-component cubic models are described in Secs. III B and III C. Section A discusses tests of the method and the accuracy achieved with short truncations.

The following notation is used for the fixed points: Gaussian, G; isotropic N-vector, $O(N)$; cubic "face" or $(1,0,0,\ldots)$ ordered, $C_f(N)$; cubic "corner" or $(1,1,1,\ldots)$ ordered, $C_c(N)$; decoupled Ising, DI; and random Ising, RI. The thermal exponent is denoted by y_{20}; it is related to the correlation-length exponent ν by $\nu=1/y_{20}$. The second largest (physical) scaling index $\dot{y}$ determines the correction-to-scaling exponent $\Delta_1= |\dot{y}| /y_{20}$, or the crossover exponent $\phi=\dot{y}/y_{20}$. Different terms are being used for singly unstable and higher-order fixed points. We have considered only even powers of the spin variable σ; however, the leading magnetic exponent y_h is related to η through $y_h =\frac{1}{2}(d +2-\eta)$.

A. General discussion

The truncated set of scaling-field equations applied to the cubic model has been defined in Sec. II. It includes the four "isotropic" fields 20, 40, 60, and 2'0 and the three "cubic" fields 04, 06, and 24. The study is for general N and dimensions $2.8 \le d \le 4$. No attempt is made to refine the calculation by studying successively longer truncations. The accuracy of the numerical results is optimized through the choice of the parameter A of Eq. (2.4). For $A = 0.5$ the isotropic N-vector critical exponents agree well with those obtained by other technqiues. Results from the scaling-field method (compared with results from the Callan-Symanzik equation[30]) for $N = 1$, 2, and 3 are $\nu = 0.631$ (0.630), 0.666 (0.669), 0.697 (0.705); $\eta = 0.024$ (0.031), 0.024 (0.033), 0.023 (0.033); and $\Delta_1 = 0.55$ (0.498), 0.58 (0.522), 0.61 (0.550), respectively.

The method has been applied to limits for which exact results are known.

(i) At $d = 4 - \epsilon$, the truncated set of equations can be solved either analytically or numerically and the results agree for $\epsilon \ll 1$. As discussed in Appendix B, the ϵ-expansion solution for the truncation reproduces the exact results to leading order in ϵ for all fixed points but the random Ising one. To obtain exact results for the latter would require an infinite set of equations. Exponents for the tricritical fixed point in $d = 3 - \epsilon$ dimensions[31] are correctly obtained to first order in ϵ.

(ii) For all N and general d, a fixed-point solution H_{DI}^* is found that corresponds to N decoupled Ising systems. The eigenvalue spectrum encompasses pure Ising exponents y^I, and exponents that can be expressed in terms of the former,[20,32]

$$y_{04}^{DI} = 2y_{20}^I - d , \tag{3.1a}$$

$$y_{06}^{DI} = 3y_{20}^I - d, \ldots , \tag{3.1b}$$

$$y_{24}^{DI} = y_{20}^I + y_{40}^I - d . \tag{3.1c}$$

Equations (3.1) provide a measure of the relative accuracy of the two sets of critical exponents. For our truncation and $d = 3$, Eq. (3.1a) is satisifed to within a factor of $\frac{4}{3}$. As discussed in Appendix A, the DI fixed point can also be used to check the computation of the coupling coefficients a_{mjk} and a_{mj}.

(iii) In the limit $N \rightarrow \infty$ the thermal exponent y_{20}^C and the correlation-function exponent η^C of the cubic fixed point $C_c(N)$ become identical with Fisher-renormalized Ising exponents[33]; i.e.,

$$y_{20}^C = y_{20}^I(1 - \alpha^I), \quad \eta^C = \eta^I . \tag{3.2}$$

This provides another test for the relative accuracy of exponents. At $d = 3$ the results from our truncation satisfy the two relations to within 5% and 25%. The result that the exponents of the isotropic $O(N)$ fixed point assume spherical-model values when $N \rightarrow \infty$,[34] is reproduced exactly. However, owing to the effects of truncation, the $1/N$ corrections are obtained only approximately.

The scaling-field method does not provide a viable method for studying critical phenomena at or near two dimensions. The truncated set of equations works well for dimensions $2.8 \le d \le 4$, but breaks down for $d \lesssim 2.8$. The reason is that as d is decreased further, the number of Gaussian operators with positive eigenvalues (2.5) increases rapidly. For example, at $d = 2\frac{2}{3}$ the operator $Q_{80}[\sigma]$, becomes relevant, which is not included in the truncation. However, relatively short truncations are appropriate for semiquantitative studies of critical phenomena for dimensions between three and four.

B. The randomly dilute Ising model

A heuristic argument by Harris,[35] together with the hyperscaling assumption, implies that small amounts of quenched impurities change the critical behavior of the Ising model to some new type for all d for which the specific-heat exponent α is positive. For dimension $d = 4 - \epsilon$ Khmelnitskii[10] and Grinstein and Luther[11] demonstrated that the new random Ising transition is described by a novel type of fixed point, now referred to as the Khmelnitskii or $\epsilon^{1/2}$ fixed point. In these works, the replica method was used.[9,11] The $\epsilon^{1/2}$ fixed point is found only for $N = 0$, for which value no cubic fixed point exists. The DI fixed point, which plays the role of the pure Ising fixed point, is unstable against "replica coupling," i.e., impurities, with a crossover exponent $\phi = \alpha^I$.[32] [This result follows from Eq. (3.1a) with $\phi = y_{04}^{DI}/y_{20}^{DI}$.] The ϵ-expansion results are inconclusive for three-dimensional systems. Since the crossover exponent is small, the question is difficult to investigate by other than RG techniques. Monte Carlo studies[36] proved inconclusive and high-temperature series expansions[37] yielded critical exponents that varied with impurity concentration.

The analysis of the weakly diluted Ising model by the scaling-field method led to the following results.

(i) A stable RI fixed point is obtained in the replica limit $N \to 0$ for all dimensions studied, $2.8 \leq d \leq 4$. This fixed point is located in the quadrant $(u < 0, v > 0)$ associated with the dilute Ising system and is accessible from the physical space by RG flow. The fixed-point structure is shown in Fig. 1(b). Consistent with the Harris argument,[35] the flow is from the DI $(u^* = 0, v^* > 0)$ towards the RI fixed point. As a function of d, the RI fixed point connects near four dimensions with the $\epsilon^{1/2}$ fixed point discussed in Appendix B. Furthermore, as shown in Figs. 1(a)−1(c) and 4, it exists
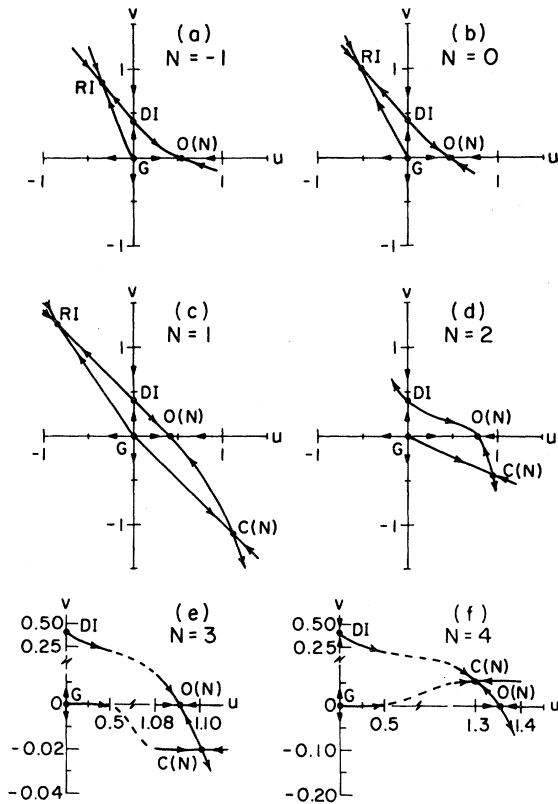

FIG. 1. Projection of the critical surface of the cubic N-vector model in three dimensions onto the plane of the isotropic and cubic coupling constants (u,v) for six values of N, as determined by the scaling-field method. (The definitions of u and v differ by a factor of 10^3 from those in the text.) The arrows on the separatrices indicate the relative stability of the isotropic $O(N)$, cubic $C(N)$, random Ising RI, decoupled Ising DI, and Gaussian G fixed points, respectively. Domains not attracted by a fixed point are interpreted as regions of first-order phase transitions. The physical subspaces are $(u > 0, v < 0)$ for the face-ordered cubic model, $(u > 0, v > 0)$ for the corner-ordered cubic model, and $(u \leq 0, v > 0)$ for the randomly dilute Ising model.

for a range of N values and, as clearly seen at $N = 1$, is distinct from the cubic $C(N)$ fixed point. This is understandable since for $N = 1$ all cubic eigenfunctionals (2.10) are zero and thus the corresponding scaling fields decouple from the Ising ones. The only physical solutions in this limit are the critical and tricritical Ising fixed points, with which the RI and $C(N)$ fixed points connect through analytic continuation. These observations raise a similar question for the three-dimensional M-vector model described by the replica limit $N = 0$ of an N,M vector model.[1,11] When $\alpha(M) > 0$, one would expect the random and "mixed" fixed points[38] to be different in three dimensions, even though they appear linked in ϵ-expansion calculations.[39]

(ii) Figures 2 and 3 present results for the thermal exponent y_{20} and correlation-function exponent η of the random and pure Ising fixed points as functions of d (solid and dashed curves, respectively). Second-order ϵ-expansion results are shown for comparison.[40,41] In Fig. 2 it is striking that the latter yield good agreement with the Ising exponents even at $d = 3$, whereas significant deviations exist for the random Ising exponents already at $d \simeq 3.9$. Also shown are pure Ising thermal exponents determined from the Kadanoff variational method for $2 < d < 4$.[42] Based on Harris's argu-
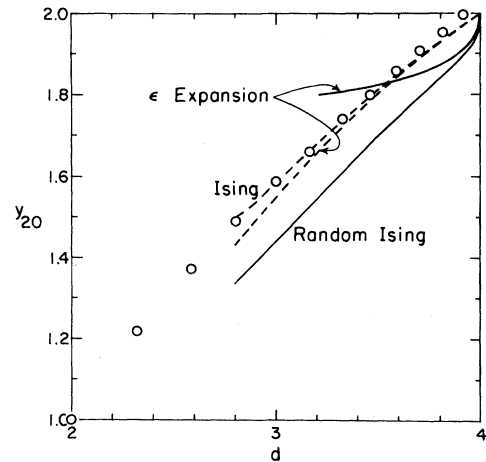

FIG. 2. Thermal exponents of the randomly dilute and pure Ising models as functions of d (solid and dashed curves, respectively) from the scaling-field method as well as extrapolations of ϵ-expansion results by Wilson (Ref. 40) and Jayaprakash and Katz (Ref. 41). The solid and dashed curves are expected to merge at $d = 2^+$. Open circles are exponents of the pure Ising model obtained by the Kadanoff variational renormalization-group method (Ref. 42).

ment, one expects new random critical behavior for this range of dimension since there $\alpha^I > 0$ or $y^I > d/2$. At the end points of this interval the random and pure fixed points probably coalesce.[43] The bow-like feature of the curves in Fig. 2 suggests that when $y^I_{20} > d/2$, then $y^{RI}_{20} < d/2$, which supports a generalization of the Harris argument.[20,44] At $d = 3$ the truncation yields $\alpha^I = 0.11$ and $\alpha^{RI} = -0.09$. The numerical results for η^{RI} are less reliable, but we expect the curves in Fig. 3 to also rejoin at $d = 2$. The change in sign in η^{RI} at $d \simeq 3.9$ was first seen in ϵ expansion.[41] The correction-to-scaling exponent is $\Delta^{RI}_1 = 0.29$.

(iii) Ising systems with both quenched and annealed impurities, such as the site-diluted Blume-Capel model,[45] are also described by the Landau Hamiltonian (1.1) in the limit $N \to 0$. This raises the interesting question of whether there exists a random tricritical[46] or random-Ising critical endpoint not yet found by ϵ expansion. Since our truncation contains only even powers of spins, it is only possible to search for a random tricritical fixed point. If one exists, it would have nonclassical exponents. (The Gaussian fixed point of the system is triply unstable.) It cannot be found with the simple truncation. Therefore, we added equa-
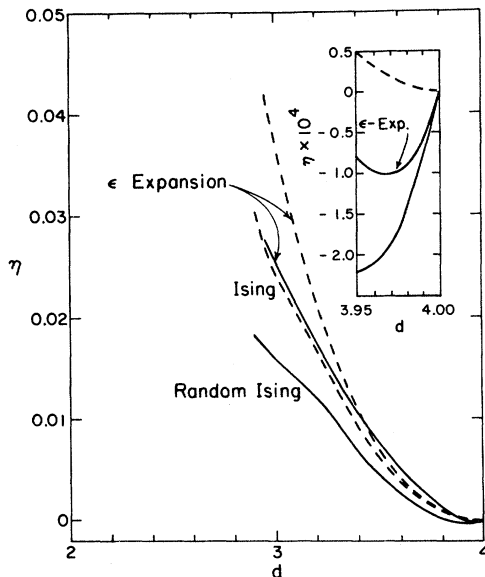

FIG. 3. Correlation-function exponent η of the randomly dilute and pure Ising models as functions of d (solid and dashed curves, respectively) from the scaling-field method and extrapolations of ϵ-expansion results (Refs. 40 and 41). The inset exhibits data near four dimensions, where the scaling-field method reproduces the ϵ-expansion results exactly for the pure Ising model, but only approximately for the dilute one.

tions for the scaling fields 80, 44, 26, 08, and 044 with $p = 0$. For $d = 3$, this truncation yielded an RG phase diagram with the right tricritical features described by a new doubly unstable fixed point. However, we think that this part of the calculation is inconclusive because the longer truncation is not well "balanced" (in the sense of Sec. II) and leads to difficulties when dimension is varied.

Experimental determination of random Ising critical exponents is difficult because the crossover exponent $\phi = \alpha^I$ is small. Various experiments have been reported.[47,48]

C. The cubic N-vector model

The cubic model (1.1) exhibits interesting crossover phenomena. From ϵ-expansion studies it is known that the stability of the isotropic $O(N)$ fixed point against a cubic field of strength v depends on the number of spin components N and spatial dimension d of the system.[3-6] Specifically, a critical value $N_c(d)$ exists such that for $N > N_c(d)$ a crossover to a cubic fixed point takes place when $v > 0$,[3] and to first-order behavior when $v < 0$.[49] The value of N_c is known for dimension $d = 4 - \epsilon$ to order ϵ^2,[4]

$$N_c(d = 4 - \epsilon) = 4 - 2\epsilon + \tfrac{5}{12}[6\zeta(3) - 1]\epsilon^2 + O(\epsilon^3)$$

(3.3)

and for dimension $d = 2 + \epsilon$ to order ϵ,[6]

$$N_c(d = 2 + \epsilon) = 2 + 4\epsilon + O(\epsilon^2) .$$

(3.4)

Obviously for $d = 3$ the physically interesting case $N = 3$ is close to N_c. The numerical value of $N_c(d = 3)$ has been controversial for some time.[19,50]

Here we report results of a study of the cubic model (1.1) for general N and dimensions $2.8 \le d \le 4$.

(i) Figures 1(d) — 1(f) display the domains of attraction and relative stability of the physical fixed points at $d = 3$ for three values of N. The value of N_c, for which the isotropic and cubic fixed points coincide, is $N_c \simeq 3.4$ for our truncation. As N is increased across N_c, the lines of isotropic and cubic fixed points cross and their stability changes; the cubic fixed point changes from tricritical $C_f(N)$ to critical $C_c(N)$ while the isotropic one changes from critical to tricritical $O(N)$. The doubly unstable fixed points are termed tricritical because there exists a special value of v, v_t, that separates regions with RG flow governed by a critical fixed point when $v > v_t$, and "runaway" flow

interpreted as indicating first-order behavior[5,29]
when $v < v_t$. For $N = 2$, the system possesses a
special symmetry in that there is no distinction be-
tween face and corner cubic order, each having
equally many ordered states. This symmetry ex-
tends to the fixed points found for $N = 2$, as shown
in Fig. 1(d). The DI and $C_f(N = 2)$ fixed-point
Hamiltonians are related through a rotation in spin
space by $\pi/4$. Both fixed points are doubly un-
stable and can be viewed as tricritical. This inter-
pretation for $C_f(N = 2)$ is consistent with the re-
sults obtained by Ditzian et al.[51] for the three-
dimensional Ashkin-Teller model.

(ii) Figures 4(a)—4(c) exhibit the exponents
versus N associated with the $C(N)$, $O(N)$, DI, and
RI fixed points at $d = 3$. The special symmetry at
$N = 2$ is apparent in all three plots. The value N_c
at which the isotropic and cubic fixed lines cross is
determined from Fig. 4(c). At N_c the exponent
$\dot{y} \equiv y_{04}$ for the $O(N)$ and $C(N)$ fixed points,
respectively, intersect and change sign. A prom-
inent feature of the curves for the thermal and
correlation-function exponents in Figs. 4(a) and
4(b) is their tangency at N_c; ϵ-expansion studies
had yielded that result for y_{20},[3] but not for η. For
$N \rightarrow \infty$, the exponents associated with the $O(N)$
and $C_c(N)$ fixed points approach the spherical
model and Fisher-renormalized Ising values,
respectively. At $N = -2$, the isotropic exponents
are Gaussian. For $N = 1$, the cubic exponents as-
sume tricritical Ising values while the random-
Ising exponents approach critical Ising values.

(iii) As a function of dimension d, the critical
value N_c varies between two and four in the inter-
val $2 \leq d \leq 4$. The pertinent information is summa-
rized in Fig. 5. Extrapolating the exact result (3.4)
near two dimensions yields the solid curve, while
the dashed curve is obtained from a Padé approxi-
mant[52] to (3.3) near four dimensions. The circles
are results for $N_c(d)$ from the scaling-field method.
The isotropic and cubic exponents were calculated
as a function of N for five dimensions in $2.8 \leq d$
≤ 4 and N_c is determined as in Fig. 4(c). Further-
more, in Ref. 19 it had been found that $N_c(d = 3)$
depends weakly on the parameter A of Eq. (2.4).
We conclude from these results that $N_c(d)$ is larger
than three at $d = 3$ and must exhibit a point of in-
flection at $d < 3$.

(iv) The evolution of the properties of the cubic
model as a function of d can be inferred from
Figs. 6 and 7. Shown are the thermal exponents
associated with the isotropic and cubic fixed points
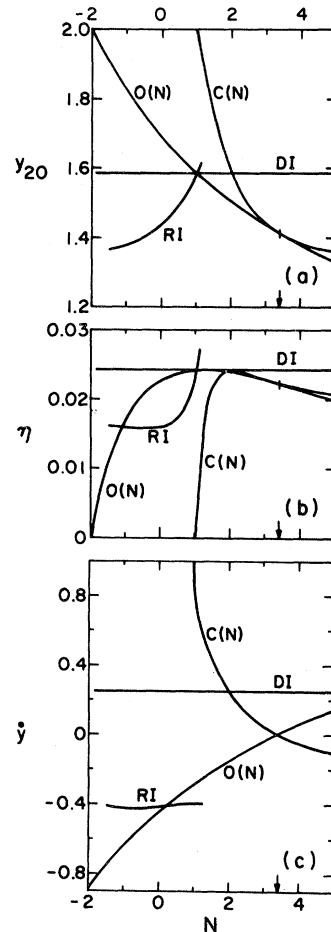as functions of N for various values of d. The

FIG. 4. Critical exponents of the cubic N-vector
model in three dimensions versus number of spin com-
ponents N for the isotropic $O(N)$, cubic $C(N)$, random
Ising RI, and decoupled Ising DI fixed points, respec-
tively, obtained by the scaling-field method. (a) Thermal
exponent y_{20} versus N. (b) Correlation-function ex-
ponent η versus N. For (a) and (b) the isotropic and cu-
bic exponents are tangent at the critical value $N_c \simeq 3.38$
and approach different limits for $N \rightarrow \infty$. (c) Exponent
$\dot{y}$ of the next-to-leading operator versus N. At
$N = N_c \simeq 3.38$, the isotropic and cubic fixed points coin-
cide and change stability.

curves for $2.8 \leq d \leq 4$ are from the scaling-field
calculation. N_c is marked by bars. Plots similar
to Fig. 4(a) may be obtained by superimposing
Figs. 6 and 7. Also shown are isotropic thermal
exponents at $d \simeq 2.32$ by Nienhuis et al.,[53] who
used Kadanoff's variational RG method; at $d = 2.1$
and 2.2 from an extrapolation of Hikami and
Brézin's $2 + \epsilon$ expansion results[54]; and at $d = 2$
from a conjecture by Cardy and Hamber.[55] The
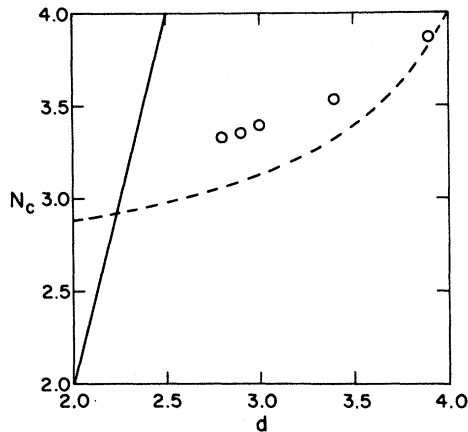exponents approach for all d the spherical-model

FIG. 5. Critical value N_c of the cubic N-vector model as function of d from the scaling-field method (open circles) and extrapolation of $2+\epsilon$ and $4-\epsilon$ expansion results (Refs. 6 and 52) (solid and dashed curves, respectively).

value $y_{20}=d-2$ at large N and the Gaussian value $y_{20}=2$ at $N=-2$. The scaling-field results for $2.8 \leq d \leq 4$ do not show the change in curvature found at small d. Less information is available for
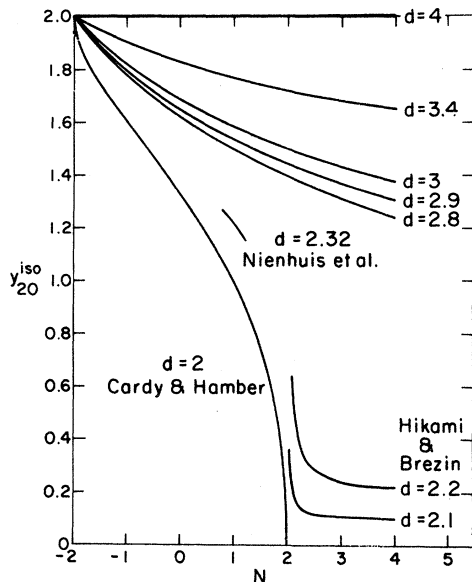

FIG. 6. Thermal exponent of the *isotropic* fixed point of the cubic N-vector model as a function of the number of spin components N and dimension d. Results from the scaling-field method between $d=4$ and 2.8 are complemented by data from Nienhuis *et al.* (Ref. 53) for $d \approx 2.32$, extrapolated ϵ-expansion results by Hikami and Brezin (Ref. 54) for $d=2.2$ and 2.1, and a conjecture by Cardy and Hamber (Ref. 55) for $d=2$.

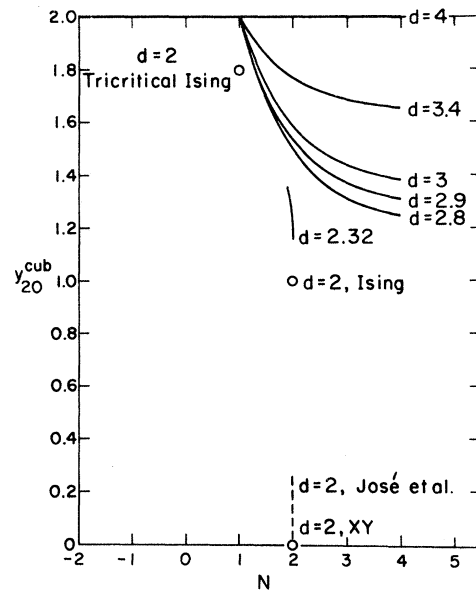
FIG. 7. Thermal exponent of the *cubic* fixed point of the cubic N-vector model as a function of the number of spin components N and dimension d. Results from the scaling-field method between $d=4$ and 2.8 are complemented by data from Nienhuis *et al.* (Ref. 53) for $d \approx 2.32$, José *et al.* (Ref. 56) for $N=d=2$, and Nienhuis *et al.* (Ref. 58) for the tricritical Ising exponent for $d=2$.

the cubic thermal exponent exhibited in Fig. 7. For all $d>2$, it assumes at $N=1$ tricritical Ising, at $N=2$ decoupled Ising, at $N=N_c$ isotropic, and at $N \rightarrow \infty$ Fisher-renormalized Ising values. Two dimensions is special. For $N=N_c=2$, we expect the exponent associated with face and corner-cubic anisotropy to vary continuously between 0 and 1, consistent with two results: First, the XY model with a weak fourfold-symmetry breaking field h_4 exhibits two branches of fixed points with $y_{20} \propto |h_4|$.[56] Second, the (discrete) Ashkin-Teller model has a continuously varying thermal exponent.[21] At $d=2$ there is no evidence yet for a $C_f(N)$ fixed point when $N<N_c$, while the $C_f(N)$ transition is first-order when $N>N_c$.[15,53] Also unresolved is the possible existence of a $C_c(N)$ fixed point when $N>N_c$ and whether it or the DI fixed point determines the critical behavior of corner-cubic systems.[57] The tricritical Ising exponent is $y_{20}=1.8$ at $d=2$.[58] The DI fixed point has a marginal eigenvalue, $\phi=\alpha^1=0$. These questions deserve further study.

In the Introduction we mentioned that the discrete cubic models are characterized by Landau Hamiltonians with perturbations of cubic and Potts

symmetry. The transition in the vicinity of the $2N$-state Potts point is known to be continuous when $2N \leq q_c(d)$ and first-order when $2N > q_c(d)$, where $q_c(d=3) < 3.$[59] For $N < N_c$, the $O(N)$ fixed point determines the critical properties of the system. For N in the window $q_c/2 < N < N_c$, we expect that the $C_f(N)$ fixed point plays the role of a tricritical fixed point separating continuous $O(N)$ from first-order phase transition behavior. As $d \to 2$, the width of the window shrinks to zero since with decreasing d, q_c increases while N_c decreases and $q_c = 2N_c$ at $d = 2$.

Structural phase transitions[7] in systems such as $LaAlO_3$, $SrTiO_3$, and $KMnF_3$ have been proposed to be in the universality class of the cubic model (1.1) with $N = d = 3.$[60] According to Fig. 1(e), the transition should be either continuous or first-order, depending upon the sign and strength of v. The experiments are in agreement with this picture. $LaAlO_3$ exhibits a corner-ordered ground state and a continuous transition.[61] Both $SrTiO_3$ and $KMnF_3$ are face-ordered, but the transitions are continuous[61,62] and first-order,[63] respectively, consistent with the fact that $KMnF_3$ is more strongly anisotropic than $SrTiO_3$.[62(b)] When the transition is continuous, the closeness of the cubic and Heisenberg exponents makes it difficult to distinguish between these types of transitions.

The value of N_c is of interest for other problems. For example, it allows one to predict details of the phase diagram of uniaxially-stressed cubic crystals[64] or the nature of the magnetic transition in cerium chalcogenides.[65]

IV. SUMMARY

The scaling-field method in critical phenomena has been generalized and applied to N-component cubic models in three dimensions, including the $N = 0$ replica limit. The technique is particularly appropriate for studying physical systems whose phase diagrams are rich in crossover phenomena. Modeling the systems by relatively short truncations yields good estimates for the asymptotic critical exponents and should provide a good starting point for computing crossover scaling functions. The method allows variation of the number of spin components N and spatial dimension d. Connection can thus be made with well understood limits such as $d = 4 - \epsilon$ and special N values.

For the random Ising model a stable random fixed point was found for the interval $2.8 \leq d \leq 4$ which, near four dimensions, is of the Khmel-

nitskii type. The simple truncation yielded at $d = 3$ the specific-heat exponents $\alpha^I \approx 0.11$ for the pure Ising and $\alpha^{RI} \approx -0.09$ for the random Ising transitions, which supports the generalized Harris argument. Analytic continuation in N showed that random Ising and cubic fixed points are distinct solutions of the scaling-field RG equations. This prompted the question in Sec. III B concerning the character of the three-dimensional random M-vector fixed point. It may be distinct from the one found by ϵ-expansion. Another open problem is the changeover from random Ising to percolative behavior at larger concentrations of impurities. The discrete corner-cubic model has the proper symmetry for formation of a percolation fixed point in the $N = 0$ limit, but is only incompletely represented by the cubic Landau Hamiltonian studied here. Also interesting is the question of the nature of the tricritical transition in a quenched randomly site-diluted Blume-Capel model. Our approximation was inadequate to answer this.

For the general cubic model, the cubic and isotropic critical exponents have been studied as functions of N and d. This allowed determination of N_c as a function of dimension. Our results in conjunction with those at $d = 2 + \epsilon$ and $4 - \epsilon$ imply $N_c(d = 3) > 3$. It may be desirable to reexamine these questions with longer truncations of scaling-field equations. Presumably this would yield critical exponents of higher precision and allow one to extend the study to $d < 2.8$. An important open question is the investigation of the full Landau Hamiltonians for the discrete face and corner-cubic models. Of interest are, for example, the relative stabilities of the cubic and Potts fixed points.

ACKNOWLEDGMENTS

APPENDIX A: COMPUTATION OF COUPLING COEFFICIENTS

The coupling coefficients a_{mjk}, a_{mj}, and a_m of Eq. (2.2) are defined by[17,66]

$$\left[\exp(P_{\sigma\tau})\int_{\vec{q}}(1+2q^2-\Delta)\frac{\delta}{\delta\vec{\sigma}(q)}\cdot\frac{\delta}{\delta\vec{\tau}(-q)}\bar{Q}_j[\sigma]\bar{Q}_k[\tau]\right]_{\vec{\tau}=\vec{\sigma}}=-\sum_m a_{mjk}\bar{Q}_m[\sigma]\ ,\tag{A1}$$

$$-\Delta\left[\exp(P_{\sigma\tau})\int_{\vec{q}}[1-2u_G^*(q)]\vec{\sigma}(q)\cdot\frac{\delta}{\delta\vec{\tau}(q)}\bar{Q}_j[\tau]\right]_{\vec{\tau}=\vec{\sigma}}-\Delta\int_{\vec{q}}\frac{\delta}{\delta\vec{\sigma}(q)}\cdot\frac{\delta}{\delta\vec{\tau}(-q)}\bar{Q}_j[\sigma]=\sum_m a_{mj}\bar{Q}_m[\sigma]\ ,\tag{A2}$$

and

$$a_m=-2A\Delta\delta_{m,2'0}\ ,\tag{A3}$$

where $\exp(P_{\sigma\tau})$ is the projection operator,

$$\exp(P_{\sigma\tau})=\exp\left[\int_{\vec{q}}[u_G^*(q)]^{-1}\frac{\delta}{\delta\vec{\sigma}(q)}\cdot\frac{\delta}{\delta\vec{\tau}(-q)}\right]\tag{A4}$$

and the $\bar{Q}[\sigma]$ are defined by Eq. (2.8). The operator (A4) contracts in all possible ways $n\,(\sigma,\tau)$ spin pairs, where $n=0,1,2,\ldots$. Thus in Eq. (A1), only projections onto polynomials $\bar{Q}_m[\sigma]$ of order $\bar{m}=\bar{j}+\bar{k}-2(n+1)$ contribute.

Similar restrictions hold for (A2). To have a simple notation for classes of projection coefficients, we denote by I the set of isotropic operators $I=\{20,40,60\}$, and by C the set of cubic operators $C=\{04,06,24\}$; the isotropic operator $2'0$ is listed separately. Two classes of projection operators vanish because of symmetry: $a_{C,II}=0$ and $a_{I,CI}=0$, as well as $a_{C,I}=a_{I,C}=0$. Therefore, we have to consider the classes $a_{I,II}$, $a_{C,CI}$, $a_{I,CC}$, and $a_{C,CC}$, as well as $a_{I,I}$ and $a_{C,C}$, plus special cases in which the I are replaced in all possible ways by $2'0$. All coupling coefficients can be written as products of combinatorial factors [number of equivalent contraction of (σ,τ) spins] times a multiple integral over momenta, which originates from the expansion of Eq. (A4) and the integral in (A1).

(i) The coefficients $a_{I,II}$ have been calculated previously and are

$$a_{\bar{m}0,\bar{j}0,\bar{k}0}=-c_{\bar{m}\bar{j}\bar{k}}I_n(d)\tag{A5}$$

with combinatorial factors $c_{\bar{m}\bar{j}\bar{k}}$ given by Eq. (3) of Ref. 17(b) (using $\hat{m}=\bar{m}/2$, $\hat{j}=\bar{j}/2$, and $\hat{k}=\bar{k}/2$) and

$$I_n=\int_{\vec{q}_1}\cdots\int_{\vec{q}_n}S(\vec{q}_1+\cdots+\vec{q}_n)\prod_{i=1}^n g(q_i)\ ,\tag{A6}$$

where $2n=\bar{j}+\bar{k}-\bar{m}-2$, with $n+1\leq\bar{j}$ and $n+1\leq\bar{k}$, and

$$S(q)=(1+2q^2-\Delta)\psi^2(q)\ ,\tag{A7}$$

$$g(q)=\psi^2(q)/u_G^*(q)\ .$$

The functions $u_G^*(q)$ and $\psi(q)$ were defined in Sec. II following Eqs. (2.4) and (2.8), respectively. The coefficient $a_{2'0,\bar{j}0,\bar{k}0}$ for even n is obtained by replacing I_n by $-J_n/(2d)$, which is defined in Eq. (A21) below. Other nonvanishing coefficients involving $2'0$ follow from (A5): $a_{2'0,2'0,20}$ for $n=0$ with I_0 replaced by 1, and $a_{(\bar{j}-2)0,\bar{j}0,2'0}$ for $n=1$ with I_1 replaced by K_1,

$$K_1=\int_{\vec{q}}(1+2q^2-\Delta)q^2\psi^2(q)g(q)\ .\tag{A8}$$

(ii) The class of coefficients $a_{C,CI}$ is given by

$$a_{\bar{m}\bar{l},0\bar{l},\bar{k}0}=\frac{-2^{n+1}(\frac{1}{2}\bar{k})!(\bar{m}+\bar{l})!}{n!\bar{k}!(\frac{1}{2}\bar{m})!(\bar{l}-n-1)!}I_n\ ,\tag{A9}$$

where $2n=\bar{k}-\bar{m}-2$ with $n+1\leq\bar{k}$ and $n+1\leq\bar{l}$; and by

$$a_{\bar{m}\bar{l},2\bar{l},\bar{k}0}=\frac{-2^{n+1}(\frac{1}{2}\bar{k})!(\bar{m}+\bar{l})!}{n!\bar{k}!(\frac{1}{2}\bar{m})!(\bar{l}-n+1)!}\left[\frac{1}{2}\bar{m}\theta(\frac{1}{2}\bar{m}-1)+\frac{n(n+1)(\frac{1}{2}N+\bar{l})\bar{l}!}{(\bar{l}+2)!}\right]I_n\tag{A10}$$

where $2n=\bar{k}-\bar{m}$, with $n+1\leq\bar{k}$ and $n+1\leq\bar{l}+2$. The coefficients $a_{C,C,2'0}$ are nonzero when $n=1$ and are obtained from Eqs. (A9) and (A10) with the integrals $I_{n=1}$ replaced by K_1 of Eq. (A8).

(iii) No general formulas exist for the classes of coefficients $a_{I,CC}$ and $a_{C,CC}$; the results are listed in Table I. The coefficients $a_{2'0,CC}$ are nonzero for even n and follow from the corresponding expressions for $a_{20,CC}$ in the table by replacing I_n by $-J_n/(2d)$, with J_n given by Eq. (A21).

The coefficients a_{mj} of Eq. (A2) are computed in a similar fashion. The nonzero a_{mj} are

$$a_{\overline{m}\overline{l},\overline{m}\overline{l}} = -(\overline{m} + \overline{l})\Delta ,$$ (A11)

$$a_{(\overline{m}-2)\overline{l},\overline{m}\overline{l}} = \frac{-2\overline{m}(\frac{1}{2}N + \frac{1}{2}\overline{m} + \overline{l} - 1)(\overline{m} + \overline{l} - 2)!}{(\overline{m} + \overline{l})!} L_1 \Delta ,$$ (A12)

with $n = 1$ and

$$L_1 = A \int_{\vec{q}} q^2 g^2(q)$$ (A13)

and

$$a_{2'0,2'0} = -2\Delta, \quad a_{2'0,20} = 4A\Delta .$$

A consistency test of the cubic coefficients of Eqs. (A9) through (A13) and Table I versus the isotropic ones of Eq. (A5) is provided by the DI fixed-point solution. Since all fixed-point coordinates are nonzero and N-dependent, this checks all coefficients.

The limit $N \to \infty$ can be performed after applying the scale transformation (2.12). The coupling coefficients $\bar{a}_{mjk}$ and $\bar{a}_{mj}$ for the equations $\bar{\mu}_m$ are obtained from

$$\bar{a}_{mjk} = N^{F_m - F_j - F_k + 1} a_{mjk}$$

and (A14)

$$\bar{a}_{mj} = N^{F_m - F_j} a_{mj} ,$$

where in the notation of (2.11) and (2.12),
$F_m \equiv F_{\overline{m}\overline{l}} = \frac{1}{2}\overline{m} + \phi_T$, etc.

It is convenient to change the normalization of the n-fold integrals I_n, etc., by a factor $[A/(2\pi)]^n$, defining $\tilde{I}_n = [A/(2\pi)]^n I_n$, etc. The scaling-field equations remain invariant by simultaneously changing $\mu \to \tilde{\mu}$,

$$\tilde{\mu}_{\overline{m}\overline{l},p} \ldots = [A/(2\pi)]^{1 - \overline{m}/2 - \overline{l}} \mu_{\overline{m}\overline{l},p} \ldots .$$ (A15)

In the remainder of this appendix we indicate how the coefficient integrals were computed for general d. First, consider the integral $\tilde{I}_n$ defined by Eq. (A6). It is simplified by writing in terms of the Fourier transforms of $S(q)$ and $g(q)$,[66]

$$\tilde{I}_n = \left[\frac{A}{2\pi}\right]^n \frac{1}{(2\pi)^d} \int_{\vec{x}} \tilde{S}(x) [\tilde{g}(x)]^n .$$ (A16)

Since $S(q)$ and $g(q)$ depend only on the magnitude of q,

$$\tilde{I}_n = \left[\frac{A}{2\pi}\right]^n \frac{\Omega_d}{(2\pi)^d} \int_0^\infty dx \, x^{d-1} \tilde{S}(x) [\tilde{g}(x)]^n ,$$ (A17)

where Ω_d is the solid angle in d dimensions

$$\Omega_d = d\pi^{d/2} / \Gamma(1 + d/2) .$$ (A18)

The simplification of (A17) over (A6) is at the expense of having to evaluate Fourier transforms to high precision. These are written

$$\tilde{S}(x) = \int_{\vec{q}} e^{i\vec{q}\cdot\vec{x}} S(q)$$

$$= \Omega_{d-1} \int_0^\infty q^{d-1} S(q) dq \int_0^\pi \sin^{d-2}\theta \, e^{iqx\cos\theta} d\theta .$$ (A19)

TABLE I. Coupling coefficients $a_{I,CC}$ and $a_{C,CC}$.

$\overline{m}\overline{l}$	20	40	04
$a_{\overline{m}\overline{l};04,04}$	$-(N-1)(N+2)I_2$	$-12(N-1)I_1$	$-6(N-2)I_1$
$a_{\overline{m}\overline{l};04,24}$	$\dfrac{-(N-1)(N+2)(N+8)I_3}{90}$	$\dfrac{-2(N-1)(N+8)I_2}{5}$	$\dfrac{-6(N-2)I_2}{5}$
$a_{\overline{m}\overline{l};04,06}$	0	0	$-2(N-2)(N+2)I_2$
$a_{\overline{m}\overline{l};24,24}$	$\dfrac{-(N-1)(N+2)(N+8)I_4}{180}$	$\dfrac{-(N-1)(N+8)(N+38)I_3}{225}$	$\dfrac{-2(N-2)(N+20)I_3}{75}$
$a_{\overline{m}\overline{l};24,06}$	0	0	$\dfrac{-8(N-2)(N+2)I_3}{15}$
$a_{\overline{m}\overline{l};06,06}$	$\dfrac{-(N-2)(N-1)(N+4)(N+8)I_4}{12}$	$\dfrac{-2(N-2)(N-1)(N+4)(N+8)I_3}{(N+2)}$	$\dfrac{-(N-4)(N-2)(N+4)^2 I_3}{(N+2)}$

Angular integration yields[67]

$$\tilde{S}(x) = \Omega_{d-1}\sqrt{\pi}\Gamma[(d-1)/2]$$

$$\times \int_0^\infty q^{d-1}S(q)$$

$$\times [2/(qx)]^{(d-2)/2}J_{(d-2)/2}(qx)dq \ .$$

$$\text{(A20)}$$

The Fourier transforms are thus obtained by performing one-dimensional integrals that contain a cylindrical Bessel function whose order depends upon dimension.

All integrals were evaluated numerically using a Newton-Cotes five-point formula.[68] The Bessel function $J_\nu(z)$ was evaluated numerically using three different types of approximation formulas for small,[69] intermediate $(z < 15)$,[70] and large z (Ref. 69); in all cases, polynomials were taken to order z^{48} or z^{-48}. There were special difficulties in evaluating $g(x)$ for $d \neq 3$. For small q, its integrand is q^{d-3} and the integral diverges logarithmically for $d \rightarrow 2$. Taylor-series expansions taken to order q^{48} were used to evaluate this integral for $0 \leq q \leq 0.1$. A test of the convergence of the final integral Eq. (A17), was provided by $n = 0$ which may be evaluated analytically, yielding $I_0 = 1$. By plotting the integrand of (A17) we observed that the small n integrals were the most difficult to evaluate. Good convergence for $n = 0$ (2 parts in 10^6) was obtained for $A = 0.5$ by integrating to $x = 40$. All numerical values are to a precision of better than 0.5%. Further checks on the method were provided by the special n and d cases where I_n can be evaluated analytically.[66] Integrals

were evaluated for dimensions $2 < d < 4$ in steps of 0.2, and a cubic spline was used to interpolate between those values.

The other integrals were calculated in a similar fashion. The integrals $\tilde{J}_n = [A/(2\pi)]^n J_n$ are obtained starting from[66]

$$\tilde{J}_n = \left[\frac{A}{2\pi}\right]^n \frac{1}{(2\pi)^d} \int_{\vec{x}} x^2\tilde{S}(x)[\tilde{g}(x)]^n \ . \quad \text{(A21)}$$

One test is provided by the analytic result

$$\tilde{J}_{n=0} = -4d\left[(2-A)-\Delta(1-A)\right] \ . \quad \text{(A22)}$$

The integrals $\tilde{K}_1$ and $\tilde{L}_1$ are single integrals that can be computed without use of Fourier transforms.

Results for the three-dimensional integrals are tabulated in Table II; the notation is $\tilde{I}_n = \tilde{I}_n'$ $+\Delta\tilde{I}_n'$. The other integrals are $\tilde{K}_1' = 0.6139$, $\tilde{K}_1'' = -0.3211$, and $\tilde{L}_1 = 1.228$, when $A = 0.5$. Values of integrals in other dimensions and coefficients for the longer truncation are available upon request.

APPENDIX B: SOLUTION BY ϵ-EXPANSION

For $d = 4 - \epsilon$, the scaling-field equations for the cubic N-vector model with $N \geq 1$ reduce in $O(\epsilon)$ to

$$\frac{d\mu_{20}}{dl} = 2\mu_{20} - \tilde{I}_2\left[\frac{(N+2)}{3N^2}\mu_{40}^2 + \frac{(N+2)(N-1)}{N^2}\mu_{04}^2\right]$$

$$-\frac{2(N+2)}{3N}\tilde{I}_1\mu_{20}\mu_{40} \ , \quad \text{(B1a)}$$

TABLE I. (Continued.)

60	24	06
$\dfrac{-120(N-1)}{(N+4)}$	$\dfrac{-180(N-2)}{(N+8)}$	$\dfrac{-20(N+2)^2}{(N+4)(N+8)}$
$\dfrac{-12(N-1)(N+8)I_1}{(N+4)}$	$\dfrac{-6(N-2)(N+20)I_1}{(N+8)}$	$\dfrac{-8(N+2)^2I_1}{(N+4)(N+8)}$
0	$\dfrac{-120(N-2)(N+2)I_1}{(N+8)}$	$\dfrac{-15(N-4)(N+4)I_1}{(N+8)}$
$\dfrac{-2(N-1)(N+8)(N+18)I_2}{5(N+4)}$	$\dfrac{-24(N-2)(N+14)I_2}{5(N+8)}$	$\dfrac{-2(N+2)^2(N+32)I_2}{15(N+4)(N+8)}$
0	$\dfrac{-2(N-2)(N+2)(N+32)I_2}{(N+8)}$	$\dfrac{-6(N-4)(N+4)I_2}{(N+8)}$
$\dfrac{-60(N-2)(N-1)(N+8)I_2}{(N+2)}$	$\dfrac{-90(N-4)(N-2)(N+4)^2I_2}{(N+2)(N+8)}$	$\dfrac{-10(N-4)(N^2+3N-16)I_2}{(N+8)}$

TABLE II. Coefficient integrals $\tilde{I}$ and $\tilde{J}$ for $d = 3$ and $A = 0.5$.

n	$\tilde{I}'_n$	$\tilde{I}''_n$	$\tilde{J}'_n$	$\tilde{J}''_n$
1	2.147	−1.505		
2	3.290[a]	−1.980	2.585	−7.185
3	4.562	−2.514		
4	6.121	−3.188	19.48[b]	−14.03
5	8.157	−4.086		
6	10.91	−5.315	35.13	−20.33

[a]Exact value $\pi^2/3$, Ref. 66.
[b]Exact value $\pi^4/5$, Ref. 66.

$$\frac{d\mu_{40}}{dl} = \epsilon\mu_{40} - \tilde{I}_1 \left[\frac{2(N+8)}{3N} \mu_{40}^2 + \frac{12(N-1)}{N} \mu_{04}^2 \right] ,$$

$$\text{(B1b)}$$

$$\frac{d\mu_{04}}{dl} = \epsilon\mu_{04} - \tilde{I}_1 \left[\frac{8}{N}\mu_{04}\mu_{40} + \frac{6(N-2)}{N} \mu_{04}^2 \right] ,$$

$$\text{(B1c)}$$

$$\frac{d\mu_{2'0}}{dl} = J_2 \left[\frac{(N+2)}{24N^2}\mu_{40}^2 + \frac{(N+2)(N-1)}{8N^2} \mu_{04}^2 \right] - 2A\Delta .$$

$$\text{(B1d)}$$

The integrals are given by $\tilde{I}_1(d=4) = \pi/(4A)$, $\tilde{I}_2(d=4) = 1.305$ for $A = 0.5$, and $\tilde{J}_2(d=4)$ $= \pi^2/(3A)$,[66] and the marginal scaling field $\mu_{2'0}^*$ is set to zero. The four fixed points of these equations; i.e., Gaussian, isotropic N-vector, decoupled Ising, and cubic N-vector have exponents y_{20}, y_{40},

y_{04}, and η that agree to leading order in ϵ with earlier results.[3]

For $N = 0$, the cubic fixed point does not exist. To study this limit we assume that the fixed-point coordinates μ_{40}^* and μ_{04}^* are of $O(\epsilon^{1/2})$ rather than $O(\epsilon)$. For consistency all terms of $O(\epsilon^{3/2})$ must be included in Eqs. (B1b) and (B1c). Within our truncation, terms of this order originate from the equations for μ_{60}, μ_{24}, and μ_{06}. This truncation exhibits a fixed point with the eigenvalues

$$y_{20} = 2 - c\epsilon^{1/2}, \quad y_{40} = -2\epsilon, \quad y_{04} = -2c(\epsilon)^{1/2}$$

$$\text{(B2a)}$$

and

$$\eta = -c^2\epsilon/12 ,$$

$$\text{(B2b)}$$

where

$$c = [6/(1296\pi^{-2}\tilde{I}_2 A^2 - 1)]^{1/2} = 0.3788 \quad \text{(B3)}$$

rather than $c = (6/53)^{1/2} = 0.3365$ found by others for the $\epsilon^{1/2}$ Khmelnitskii fixed point.[11,41,71] One suspects correctly that there are other terms of $O(\epsilon^{3/2})$ not included in the truncation. Unfortunately, it turns out that there is an infinite number of equations and terms that have to be added: specifically, all fields $\mu_{\overline{ml};p} \ldots$ with $p \geq 2$ and $\overline{ml}$ up to sixth order in spin. Our conclusion is that the scaling-field method is not appropriate for ϵ-expansion calculations requiring terms beyond the leading order ones. Other approaches are not plagued by this problem. In fact, one can show that classes of coupling constants vanish when the sharp cutoff limit is taken on Wilson's incomplete integration formula.[72]

---

*Present address: Department of Physics, University of Illinois, Urbana, Ill. 61801.

[1]A. Aharony, in *Phase Transitions and Critical Phenomena*, edited by C. Domb and M. S. Green (Academic, London, 1976), Vol. 6, p. 357.
[2]M. E. Fisher, Rev. Mod. Phys. <u>46</u>, 597 (1974).
[3]A. Aharony, Phys. Rev. B <u>8</u>, 4270 (1973).
[4]I. J. Ketley and D. J. Wallace, J. Phys. A <u>6</u>, 1667 (1973).
[5]J. Rudnick, Phys. Rev. B <u>18</u>, 1406 (1978), and references therein.
[6]R. A. Pelcovits and D. R. Nelson, Phys. Lett. A <u>57</u>, 23 (1976).
[7]A. D. Bruce, Adv. Phys. <u>29</u>, 111 (1980), and references therein.
[8]D. Kim, P. M. Levy, and L. F. Uffer, Phys. Rev. B <u>12</u>, 989 (1975).
[9]V. J. Emery, Phys. Rev. B <u>11</u>, 239 (1975).
[10]D. E. Khmelnitskii, Zh. Eksp. Teor. Fiz. <u>68</u>, 1960 (1975) [Sov. Phys.—JETP <u>41</u>, 981 (1976)].
[11]G. Grinstein and A. Luther, Phys. Rev. B <u>13</u>, 1329 (1976).
[12]T. C. Lubensky, in *Ill-Condensed Matter* (Les Houches, Session XXXI, 1978), edited by R. Balian, R. Maynard, and G. Toulouse (North-Holland, Amsterdam, 1979), p. 407.
[13]A. Aharony, J. Phys. A <u>10</u>, 389 (1977).
[14]E. Domany and E. K. Riedel, Phys. Rev. B <u>19</u>, 5817 (1979).
[15]E. K. Riedel, Physica A <u>106</u>, 110 (1981).
[16]K. G. Wilson and J. Kogut, Phys. Rep. <u>12C</u>, 75 (1974), especially Sec. 11 and Appendix A.

[17](a) G. R. Golner and E. K. Riedel, Phys. Rev. Lett. 34, 856 (1975); (b) Phys. Lett. A 58, 11 (1976).

[18]F. J. Wegner, in *Phase Transitions and Critical Phenomena,* edited by C. Domb and M. S. Green (Academic, London, 1976), Vol. 6, p. 7. This paper contains reviews of the Wilson RG equation and the scaling-field method.

[19]E. Domany and E. K. Riedel, J. Appl. Phys. 50, 1804 (1979).

[20]S. K. Ma, *Modern Theory of Critical Phenomena* (Benjamin, Reading, Massachusetts, 1976), Chap. X.

[21]J. Ashkin and E. Teller, Phys. Rev. 64, 178 (1943); F. Wegner, J. Phys. C 5, L131 (1972); L. P. Kadanoff and F. J. Wegner, Phys. Rev. B 4, 3989 (1971).

[22]J. B. Hubbard, Phys. Lett. A 39, 365 (1972).

[23]S. Krinsky and D. Mukamel, Phys. Rev. B 16, 2313 (1977). See also L. D. Landau and E. M Lifshitz, *Statistical Physics* (Addison-Wesley, Reading, Massachusetts, 1969), Chap. XIV.

[24]P. W. Kasterleyn and C. M. Fortuin, J. Phys. Soc. Jpn. (Suppl.) 16, 11 (1969).

[25]R. Bidaux, J. P. Carton, and G. Sarma, J. Phys. A 9, L87 (1976); D. J. Wallace and A. P. Young, Phys. Rev. B 17, 2384 (1978).

[26]H. Bateman, *Higher Transcendental Functions* (McGraw-Hill, New York, 1953), Vol. II.

[27]K. E. Newman and E. K. Riedel, unpublished.

[28]T. L. Bell and K. G. Wilson, Phys. Rev. B 11, 3431 (1975).

[29]See also H. H. Iacobson and D. J. Amit (unpublished); T. A. L. Ziman, D. J. Amit, G. Grinstein, and C. Jayaprakash (unpublished).

[30]J. C. Le Guillou and J. Zinn-Justin, Phys. Rev. B 21, 3976 (1980). See also G. A. Baker, B. G. Nickel, and D. I. Meiron, Phys. Rev. B 17, 1365 (1978).

[31]M. J. Stephen and J. L. McCauley, Phys. Lett. A 44, 89 (1973).

[32]J. Sak, Phys. Rev. B 10 3957 (1974).

[33]A. Aharony, Phys. Rev. Lett. 31, 1494 (1973).

[34]H. E. Stanley, Phys. Rev. 176, 718 (1968).

[35]A. B. Harris, J. Phys. C 7, 1671 (1974).

[36]D. P. Landau, Phys. Rev. B 22, 2450 (1980).

[37]D. C. Rapaport, J. Phys. C 5, 2813 (1972); G. S. Rushbrooke, R. A. Muse, R. L. Stephenson, and K. Pirnie, *ibid.* 5, 3371 (1972); M. A. A. Cox, J. W. Essam, and C. M. Place, *ibid.* 9, 1719 (1976).

[38]A. B. Harris and T. C. Lubensky, Phys. Rev. Lett. 33, 1540 (1974); T. C. Lubensky, Phys. Rev. B 11, 3573 (1975).

[39]For $N = 1$ the "mixed" N, M fixed point is tricritical. As N is decreased, the fixed-point coordinates move through infinity and, at $N = 0$, the "random" fixed point is critical. For $M \neq 1$, both fixed points are of $O(\epsilon)$.

[40]K. G. Wilson, Phys. Rev. Lett. 28, 548 (1972).

[41]C. Jayaprakash and H. J. Katz, Phys. Rev. B 16, 3987 (1977).

[42]S. L. Katz, M. Droz, and J. D. Gunton, Phys. Rev. B 15, 1597 (1977).

[43]See, however, Vik. S. Dotsenko and Vi. S. Dotsenko, unpublished.

[44]Note, however, the results of Ref. 41 imply that $\mathring{y}^{RI}$ and α^{RI}/ν^{RI} are unequal but have the same sign.

[45]M. Blume, Phys. Rev. 141, 517 (1966); H. W. Capel, Physica (Utrecht) 32, 966 (1966).

[46]M. J. Stephen, Phys. Lett. A 55, 273 (1975); Phys. Rev. B 13, 2007 (1976). See also comments in A. Aharony, J. Magn. Magn. Mater. 7, 198 (1978).

[47]E. Lagendijk and W. J. Huiskamp, Physica (Utrecht) 62, 444 (1972).

[48]R. A. Dunlap and A. M. Gottlieb, Phys. Rev. B 23, 6106 (1981); R. A. Cowley and K. Carneiro, J. Phys. C 13, 3281 (1980).

[49]D. J. Wallace, J. Phys. C 6, 1390 (1973).

[50]M. K. Grover, L. P. Kadanoff, and F. J. Wegner, Phys. Rev. B 6, 311 (1972); F. J. Wegner, *ibid.* 6, 1891 (1972); M. C. Yalabik and A. Houghton, Phys. Lett. A 61, 1 (1977).

[51]R. V. Ditzian, J. R. Banavar, G. S. Grest, and L. P. Kadanoff, Phys. Rev. B 22, 2542 (1980).

[52]D. R. Nelson, J. M. Kosterlitz, and M. E. Fisher, Phys. Rev. Lett. 33, 813 (1974).

[53]B. Nienhuis, E. K. Riedel, and M. Schick (unpublished).

[54]S. Hikami and E. Brézin, J. Phys. A 11, 1141 (1978).

[55]J. Cardy and H. Hamber, Phys. Rev. Lett. 45, 499 (1980).

[56]J. V. José, L. P. Kadanoff, S. Kirkpatrick, and D. R. Nelson, Phys. Rev. B 16, 1217 (1977).

[57]See also G. S. Grest and M. Widom, unpublished.

[58]B. Nienhuis, N. Berker, E. K. Riedel, and M. Schick, Phys. Rev. Lett. 43, 737 (1979).

[59]B. Nienhuis, E. K. Riedel, and M. Schick, Phys. Rev. B 23, 6055 (1981), and references therein.

[60]R. A. Cowley and A. D. Bruce, J. Phys. C 6, L191 (1973); A. D. Bruce, *ibid.* 7, 2089 (1974).

[61]K. A. Müller and W. Berlinger, Phys. Rev. Lett. 26, 13 (1971).

[62](a) T. von Waldkirch, K. A. Müller, W. Berlinger, and H. Thomas, Phys. Rev. Lett. 28, 503 (1972); (b) T. von Waldkirch, K. A. Müller, and W. Berlinger, Phys. Rev. B 7, 1052 (1973).

[63]K. Gesi, J. D. Axe, G. Shirane, and A. Linz, Phys. Rev. B 5, 1933 (1973).

[64]A. Aharony and A. D. Bruce, Phys. Rev. Lett. 33, 427 (1974); A. D. Bruce and A. Aharony, Phys. Rev. B 11, 478 (1975).

[65]D. Mukamel and D. J. Wallace, J. Phys. C 12, L851 (1979).

[66]E. K. Riedel, G. R. Golner, and K. E. Newman (unpublished).

[67]I. S. Gradshteyn and I. W. Ryzhik, *Table of Integrals, Series and Products* (Academic, New York, 1965), p. 482.

[68]F. B. Hildebrand, *Introduction to Numerical Analysis* (McGraw-Hill, New York, 1974), p. 73.

[69]*Handbook of Mathematical Functions,* edited by M. Abramowitz and I. A. Stegun, Natl. Bur. Stand. Appl. Math. Series, No. 55 (U. S. GPO, Washington, D. C., 1965), Chap. 10.

[70]Y. L. Luke, *Algorithms for the Computation of*

Mathematical Functions (Academic, New York, 1977), p. 203.

[71]A. Aharony, Phys. Rev. B 13, 2092 (1976).

[72]K. E. Newman (unpublished).